Impact Monitoring of Embedded Batteries in Sandwich Composites with Integrated Soft Elastomeric Capacitors

Emmanuel A. Ogunniyi[a], Austin R.J. Downey[a,b], Han Liu[c], Simon Laflamme[c,d], and Subramani Sockalingam[a]

[a]Department of Mechanical Engineering, University of South Carolina, Columbia, USA
[b]Department of Civil and Environmental Engineering, University of South Carolina, Columbia, USA
[c]Department of Civil, Construction, and Environmental Engineering, Iowa State University, Iowa, USA
[c]Department of Electrical and Computer Engineering, Iowa State University, Iowa, USA

ABSTRACT

Flexible sensors such as soft elastomeric capacitors (SECs) can be integrated into composite materials like fiberglass as a method to directly monitor embedded batteries during an impact event. In high-performance applications, where impact damage can result in catastrophic battery failures, including fires or explosions, the use of highly sensitive sensors is critical for ensuring the safety and reliability of composite structures. SECs have been widely used in modern health monitoring under diverse applications, offering adjustable sensitivity to detect even minute changes in structural states. These thin-film, flexible sensors are highly compliant and scalable, allowing them to conform to curved surfaces and complex geometries, such as those of batteries. Their flexibility addresses the limitations of conventional sensors, which may miss critical impact events. This study explores the use of SECs to monitor, detect, and quantify impact energy directly on batteries embedded within sandwich composites. The SEC is attached directly to the battery surfaces and embedded within the sandwich composite material, then subjected to controlled impact tests using a drop weight testing machine. The experimental setup evaluates the performance of SECs in measuring impact energy at varying impact levels while also examining the effects of the impacts on the embedded batteries' charge and discharge capacities. By advancing the understanding of flexible capacitors and their applications in sensing technologies, this study demonstrates the viability of SECs as effective sensors for real-time impact energy monitoring, highlighting the potential of SECs to enhance the safety of composite materials with embedded batteries in high-risk environments.

Keywords: Soft Elastomeric Capacitors (SECs), impact energy monitoring, battery, composite materials, flexible sensors, impact detection, structural health monitoring (SHM)

1. INTRODUCTION

The rising demand for safer, more reliable energy storage systems in high-performance sectors such as electric vehicles, aerospace, and defense stems from increasing reliance on battery-powered technologies.[1] As industries push for lighter, energy-dense systems, the risk of battery failure under extreme conditions, for example impacts or crashes, becomes a critical concern, with the potential for catastrophic outcomes like thermal runaway, explosions, or fires.[2] Ensuring battery integrity and reliability under hazardous conditions is a priority for researchers, especially given high-profile failures in consumer electronics and industrial applications. In sectors like aviation, space exploration, and defense, where batteries face extreme mechanical stress, impact damage can compromise both energy storage and overall structural integrity, risking mission-critical failures.[3,4] This highlights the need for real-time monitoring technologies to detect impact energy, predict failures, and prevent catastrophic incidents.

Send correspondence to Austin R.J. Downey
Austin R.J. Downey: Email: austindowney@sc.edu

Composite materials have emerged as a leading choice for battery encasement in high-performance applications due to their superior mechanical properties, including high strength-to-weight ratios, resistance to environmental degradation, and flexibility in design.[5,6] Fiberglass, in particular, provides excellent energy absorption during impacts, making it an ideal protective layer for critical components like batteries.[7] However, despite these advantages, challenges lie in the real-time monitoring of impact events and the subsequent structural changes that could compromise the integrity and safety of the system. Traditional impact monitoring solutions, such as piezoelectric and resistive strain sensors, often suffer from limitations such as rigidity, low sensitivity to minor deformations, and inadequate coverage over curved or complex geometries.[8] These shortcomings can lead to missed detections of subtle yet critical impact events, which could escalate into larger structural failures or undetected internal battery damage. Therefore, there is a need for advanced sensing solutions that not only integrate seamlessly with the composite material but also provide accurate, continuous monitoring of impact energy and structural health.

Soft elastomeric capacitors (SECs) have gained attention due to their unique combination of flexibility, thin-film design, and high sensitivity.[9,10] SECs can conform to complex geometries, making them particularly suited for monitoring curved or irregular surfaces.[11] Additionally, their sensitivity can be tuned to detect even minor deformations, providing a critical advantage in applications where early detection of structural changes is crucial. SECs have already demonstrated their effectiveness in a variety of SHM applications, including monitoring strain in flexible electronics, detecting structural deformations in aerospace components, and assessing the performance of wearable devices. These capabilities position SECs as a promising candidates for addressing the specific challenges associated with battery impact monitoring. Furthermore, their thin and lightweight design ensures minimal intrusion into the composite material's structural properties, allowing for seamless integration without compromising mechanical performance.

Despite the progress made in SEC-based SHM systems, their application for directly monitoring impact energy[12] on batteries embedded within composite materials is yet to be explored. This gap presents a significant research opportunity to develop and validate SECs as a real-time sensing solution tailored for such critical applications. Specifically, integrating SECs into sandwich composites could provide a transformative approach for monitoring and quantifying impact energy, enabling detailed insights into how different levels of mechanical stress affect battery performance and structural integrity.[13] This type of real-time monitoring is especially valuable for identifying early signs of damage, such as microcracks or delaminations, that could compromise the safety and functionality of the battery system.[14] Moreover, addressing this research gap aligns with the broader trend toward predictive maintenance and smart monitoring systems in high-performance applications.

This study investigates the integration of SECs into sandwich composites for the purpose of real-time monitoring, detection, and measurement of impact energy on embedded batteries. The experimental methodology employs a drop-weight impact testing machine to simulate varying levels of mechanical stress, enabling a systematic evaluation of SECs and their response to real-world impact conditions. During the impact test, a controlled weight is dropped from varying heights onto the sandwich composite specimens embedded with SEC and LiPo battery. This setup ensures a consistent and reproducible application of impact energy, allowing for a detailed analysis of the relationship between the induced mechanical stress on the structure and the electrical responses of the system. Following each impact, the structural integrity of the composite is assessed. These provide a clear visualization of the extent and geometry of the internal damage caused by the impact, facilitating a thorough understanding of how different impact energies affect the composite material. In addition to studying the impact's mechanical effects, the electrochemical performance of embedded batteries is observed after each impact. The batteries undergo a series of charge and discharge cycles before and after each impact event, with key parameters such as capacity and voltage recorded. This process evaluates how impact-induced mechanical stresses influence the electrochemical behavior of the batteries, offering valuable insights into their long-term reliability and performance under dynamic conditions. The study provides a holistic understanding of the system's performance by correlating changes in the battery's charge and discharge characteristics with observed damage patterns and SEC responses.

The contributions of this paper lies in 1) demonstrating the feasibility of using SECs for impact energy detection in embedded batteries; 2) the development of smart, self-monitoring composite material, as such materials could significantly enhance the safety and performance of various systems, including electric vehicles, aerospace components, and renewable energy storage, where the risk of mechanical failure must be mitigated to ensure operational success.

2. BACKGROUND

2.1 Energy Storage Composite

Energy storage composites represent a cutting-edge approach in material science, merging structural functionality with energy storage capabilities.[15] These multifunctional materials directly integrate energy storage devices, such as batteries or supercapacitors, into composite structures, enabling systems to maintain high mechanical strength while providing power. This dual role is particularly beneficial in high-performance applications like aerospace, automotive, and renewable energy systems, where weight reduction and spatial efficiency are critical. By embedding batteries within composite materials, energy storage composites reduce the reliance on standalone battery modules, thus optimizing the overall system design. Despite their advantages, integrating batteries into structural components poses significant challenges. These include potential reductions in mechanical properties such as stiffness,[16] vibration damping,[17] and fatigue resistance.[18] However, advancements in design methodologies and manufacturing processes have demonstrated that these mechanical drawbacks can be mitigated or even eliminated. Recent studies have shown that optimizing the bonding between the battery and the composite structure can minimize mechanical degradation, allowing the composite to retain its load-bearing capacity under operational stresses.[19]

Fiberglass and carbon fiber are the most widely used materials for structural composites due to their high strength-to-weight ratio and durability. Fiberglass, in particular, offers excellent flexibility and energy absorption, making it a preferred choice for embedding energy storage systems. Research efforts are focused on improving these materials' mechanical and electrochemical integration to enhance their operational durability.[20,21] By addressing challenges related to thermal management, load distribution, and long-term stability, energy storage composites can revolutionize structural health monitoring (SHM) and safety in next-generation energy systems.[7]

2.2 Soft Elastomeric Capacitors

Soft elastomeric capacitors (SECs) have emerged as a promising sensor technology in SHM due to their flexibility, high sensitivity, and environmental robustness.[22] These sensors operate as parallel plate capacitors, utilizing an elastomeric dielectric material that can stretch significantly under strain without yielding. SECs have proven highly effective in monitoring a wide range of structural behaviors, including detecting fatigue cracks in steel[23] and measuring strain in concrete structures.[24]

The key material used in SECs is styrene-ethylene-butylene-styrene (SEBS), an elastomer capable of stretching up to 500% of its original dimensions while maintaining a linear response within its sensing range. SECs can measure strains as small as 25 $\mu\epsilon$, making them particularly useful in applications requiring high precision. The dielectric layer of the SEC is created by dispersing titania within the SEBS matrix, while the conductive plates are formed by mixing carbon black (CB) particles into the SEBS, producing a conductive network. These conductive layers are applied in thin films over the dielectric, resulting in sheet resistance of approximately 1 kΩ.[9]

The CB-SEBS composite enhances the sensor's electrical properties and provides considerable environmental durability, enabling SECs to function effectively in harsh operating conditions. Additionally, SECs are equipped with copper contacts to interface seamlessly with data acquisition systems, ensuring reliable performance during long-term monitoring. Their lightweight, flexible design and scalability make SECs attractive for integrating real-time sensing capabilities into composite structures.

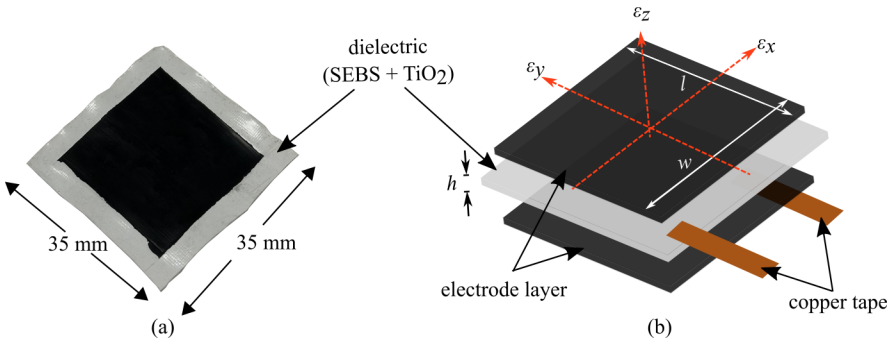

Figure 1. Soft elastomeric capacitor where (a) is a 35 mm × 35 mm ($l \times w$) SEC ; and (b) is the schematic showing the parallel plate capacitor structure of the SEC with key components and reference axes annotated.

2.2.1 Sensor Model

Equation 1 presents the parallel plate capacitor formulation used to model the electrical properties of the SEC in terms of its physical qualities. The capacitance C is associated with the ratio of the area of the conductive plates, $l \cdot w$, to the distance d between the plates, scaled by the vacuum permittivity ϵ_0 and the relative permittivity of the dielectric ϵ_r,

$$C = \epsilon_0 \epsilon_r \frac{l.w}{d} \tag{1}$$

The change in capacitance of the SEC, as expressed in Equation 2 and illustrated in Figure 1, can be obtained by taking the gradient of the capacitance expression in Equation 1. The Δ operator represents aggregation over a discrete sensor volume, while the gradient operator ∇ suggests a sum of partial derivatives in three orthogonal axes of the material.

$$\nabla C = \epsilon_0 \epsilon_r \left(\frac{l}{d} \partial w + \frac{w}{d} \partial l - \frac{lw}{d^2} \partial d \right) \approx \epsilon_0 \epsilon_r \left(\frac{L}{d} \Delta w + \frac{W}{d} \Delta l - \frac{lw}{d^2} \Delta d \right) \tag{2}$$

Equation 2 displays a discrete volume that can be used to approximate the derivative for homogeneous small strains within the sensor. Equation 3, which directly links strains to variations in sensor capacitance, is obtained by normalizing this slight change by the original capacitance.

$$\frac{\Delta C}{C_0} = \frac{\Delta w}{w} + \frac{\Delta l}{l} - \frac{\Delta d}{d} = \epsilon_w + \epsilon_l - \epsilon_d \tag{3}$$

Equation 5 is obtained by using Hooke's stress-strain relationship under the plane stress assumption and replacing ϵ_d in Equation 3 with the definition in Equation 4.

$$\epsilon_d = -\frac{\nu}{E} (\sigma_l + \sigma_w) = -\frac{\nu}{1-\nu} (\epsilon_l + \epsilon_w) \tag{4}$$

$$\frac{\Delta C}{C_0} = \frac{1}{1-\nu} (\epsilon_w + \epsilon_l) \tag{5}$$

This gives the sensor's capacitance change relative to changes in the material state.[25]

2.2.2 Impact model

The ability of a material to absorb strain energy without permanently deforming is known as proof of resilience. When this threshold is exceeded, energy is stored as a nonconservative loss. The strain energy retained in the plate due to hits above the threshold for plastic deformation can be measured by tracking mechanical energy losses. By keeping an eye on the impactor's impact velocity and the force measured by its load cell, one can ascertain how much energy the plate has absorbed.[26]

$$E_{\text{sys}}(t) = T_{\text{kinetic}}(t) + U_{\text{gravitational}}(t) - U_{\text{strain}}(t) = 0 \tag{6}$$

The simplification shown in Equation 6 is valid during the observation of the impact event from the moment of contact until the impactor leaves the sample, with small losses attributable to ambient interactions being ignored.

$$\Delta U_{\text{strain}} = \Delta T_{\text{kinetic}} + \Delta U_{\text{gravitational}} \tag{7}$$

Equation 7 shows that the entire change in the impactor's mechanical energies during contact with the composite plate is equal to the total energy stored in the plate (ΔU_{strain}). The integration of the load cell signal causes the impactor's change in momentum. Equation 8 shows how to obtain the momentum scaling by the mass of the impactor velocities.

$$\Delta U_{\text{strain}} = m\left(\frac{V_f^2 - V_i^2}{2}\right) + mg\Delta h \tag{8}$$

Here, V_i and V_f represent the impactor's velocities before and after the impact event. Furthermore, m represents the impactor's mass, g the acceleration caused by gravity, and Δh the change in the impactor head's height.

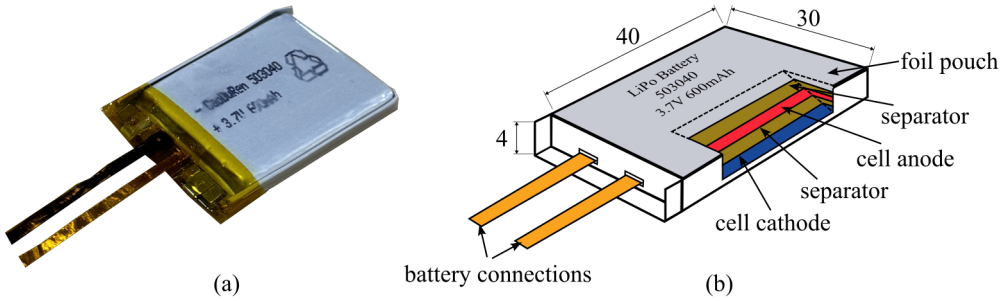

Figure 2. The battery embedded within the sandwich composite where (a) LiPo battery, and; (b) is the schematic of LiPo battery components and dimensions (in mm).

3. METHODOLOGY

3.1 Multifunctional Energy storage Composites

The exact image and schematic of the LiPo battery, which was acquired from the supplier and is safely embedded in a thin-film protective aluminum pouch, are shown in Figures 2(a) and (b). The SEC was attached to the battery's surface using bi-component epoxy before it was embedded in the composite. The battery has a 600 milliampere-hour (mAh) capacity and operates at a voltage of 3.7 volts, with a voltage range of 2.7 to 4.2 volts. Copper tapes measuring 80 mm in length and 4 mm in width were used to connect the batteries. These tapes are sufficiently flat to be inserted between the sandwich composite without adding additional thickness to the sample. This arrangement enabled charging, discharging, and electrical testing to be performed on them before the batteries were integrated into the composites. Additionally, it made it possible to do additional testing following the embedding of the batteries and any impact.

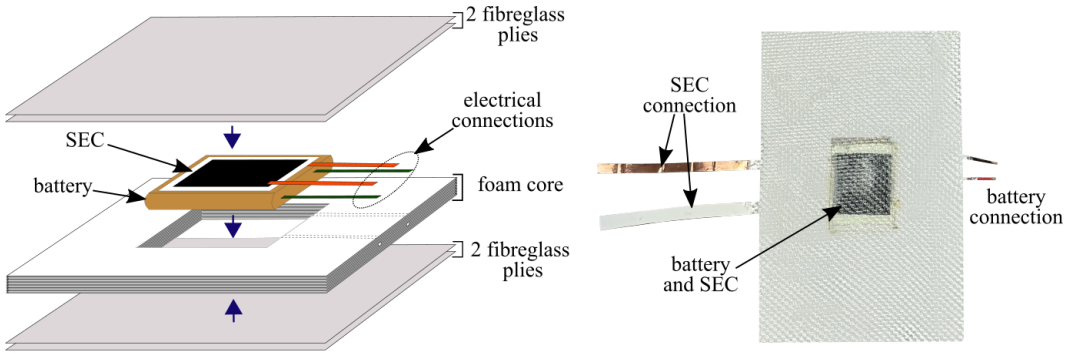

Figure 3. Sandwich composite where (a) shows the schematic of the sample indicating the embedding process, and; (b) is the cured sandwich composite with battery and SEC embedded.

The sandwich composite structure comprises a PVC foam core with a density of 100 kg/m^3 and fiberglass laminate face skins. Two layers of laminates oriented in a [0/90]s orientation were used to form the surface skins. A 40 mm x 30 mm rectangular hole precisely matching the battery's size was carved into the foam core to hold the battery with attached SEC. The battery was inserted so that its top and bottom surfaces could be directly touched with the inner sides of the laminate skins. The foam core completely encased the battery's 4 mm thick sidewalls, preventing interference with the surface skins' ability to support loads. Figures 3(a) describe the schematic of the sandwich composite material. The fiberglass skins were made utilizing epoxy resin in a wet hand lay-up procedure. The resin attached the skins to the foam core after curing without needing an extra layer of glue, and the entire sandwich structure was allowed to cure at ambient temperature as shown in Figures 3(b). The composite thickness was 5.5 mm, as the thickness of each laminate skin was 0.75 mm, and the foam core was 4 mm thick.

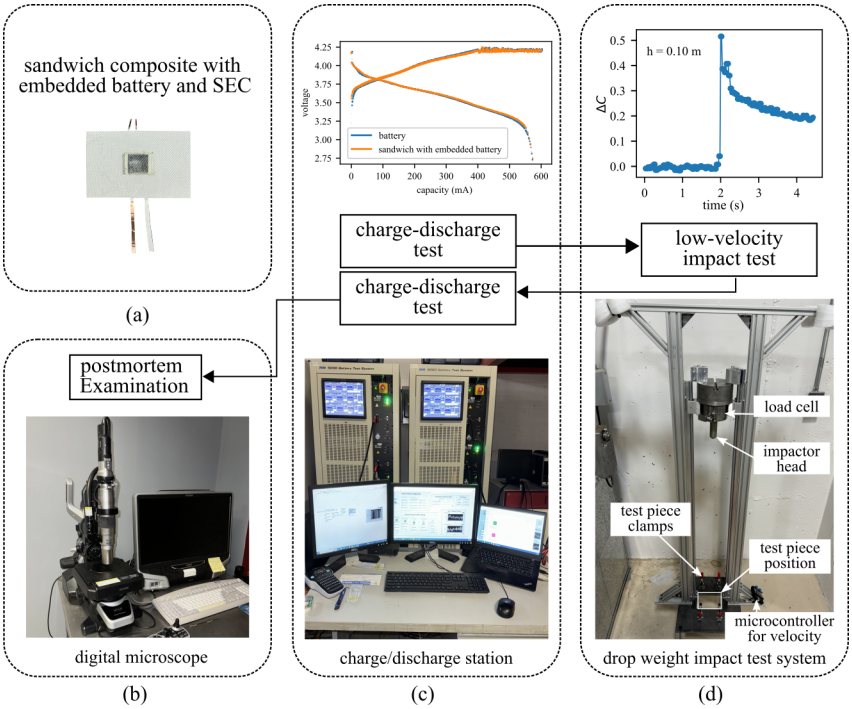

Figure 4. Experimental process showing (a) sandwich composite with battery and SEC embedded; (b) digital microscope used for observing extent of damage on the samples; (c) charge/discharge test station, and; (d) drop weight impact test setup.

3.2 Charge and discharge tests

Impact loading can cause minor damage to embedded batteries, such as mechanical harm to separators or electrodes, which may degrade electrochemical performance without causing catastrophic failures like heat generation or internal short circuits. Charge-discharge cycle experiments were performed before and after the impact testing to assess the embedded pouch cells' capacity loss and performance deterioration. The embedded batteries, integrated into the sandwich composite samples, were cycled using a constant-current, constant-voltage (CCCV) scheme at 1C (600 mAh) using a NHR 9200 battery test system in Figures 4(c). Voltage limits were set between 4.2 V and 2.75 V, with a C/30 cutoff. During the cycling process, key metrics, including cell capacity, internal resistance, voltage, and current, were recorded at 10-second intervals to track performance over time.

3.3 Impact tests

The drop tower used for the impact tests was constructed by ASTM standards as shown in Figures 4(d), except for the impactor mass, which was non-standard at 7.5 kg. A pancake-type Honeywell Model 43 load cell, compliant with ASTM D7136/D7136M, was used to record impact forces at a sampling rate of 15 kHz. The test specimens measuring 150 mm in length and 100 mm in width were placed on an unsupported base (137.5 mm $\times$ 87.5 mm) with fully clamped edges. The embedded battery was positioned at each specimen's center as the designated impact point. Each specimen was impacted once, and the rebound was controlled to prevent additional impacts to ensure consistency. Impact velocity and kinetic energy were measured using a sensor on the impact rig and verified by applying the energy balance equation based on potential energy from the measured drop height. This approach allowed the work done on the composite plate during impact to be calculated and compared to the measured capacitance change of the SEC. Capacitance measurements were collected using a B&K Precision Model 891 LCR meter, operating at a test frequency of 1 kHz and a sampling frequency of 45 samples per second. For safety, all embedded batteries were pre-charged to 60% state of charge (SOC) prior to testing. Impact tests were conducted at heights 0.05, 0.10, 0.12, 0.15 m, and 0.20 m, corresponding to energy levels of 3.7, 7.4, 8.8, 11.0, and 14.7 J, with each energy level repeated twice to ensure the reproducibility of results. The upper limit for impact energy on the sample was set at 14.7 J to prevent battery exposure on the specimen surface.

A microscope (Figures 4(b)) was used to examine the sandwich composite samples before and after impact testing. Impact damage was measured using indentation depth and the estimated surface damage area between the fiberglass layers and the LiPo battery. Around the damage, the estimated surface damage was measured. The indentation depth was calculated by measuring from the top of the intact face sheet to the place on the impacted face sheet that was most badly damaged.

4. RESULTS

This section presents the results of the study, including charge/discharge testing of the embedded sandwich composite both before and after impact, impact testing of the sample, and associated energy calculations.

4.1 Charge/Discharge before impact

Figures 5(a) illustrates the charge/discharge voltage profiles of a bare LiPo battery and the battery embedded within a sandwich composite material integrated alongside an SEC. Both configurations exhibit a similar voltage-capacity relationship, indicating consistent electrochemical performance across charge and discharge cycles. The capacity retention for both setups remains nearly identical, demonstrating that embedding the battery within the composite does not significantly affect its overall energy storage capability. These results highlight the feasibility of integrating batteries into composite structures without substantial performance degradation, which is critical for applications requiring multifunctional, embedded energy solutions.

4.2 Impact test on embedded sandwich composite

Figure 6 illustrates the response of a sandwich composite sample with embedded SEC and battery subjected to impacts from various heights, specifically analyzing capacitance change (ΔC) (Figure 6(a)-(e)), extent of damage (Figure 6(f)-(j)), and the corresponding force recorded by a load cell (Figure 6(k)-(o)). The impact heights considered are 0.05, 0.10, 0.12, 0.15 m, and limited to 0.20 m to prevent exposure of the battery that

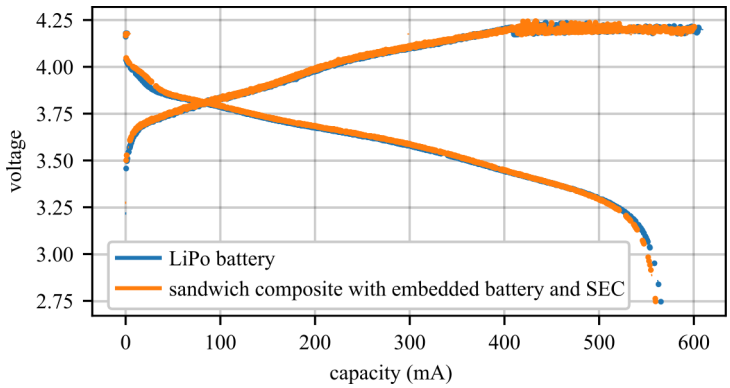

Figure 5. Charge/discharge test comparison between the LiPo battery and the sandwich composite with embedded SEC and battery.

Table 1. Impact Test data on sandwich composite sample

Impact Height (m)	ΔC (pF)	Peak Force (N)	Indentation Depth (mm)
0.05	0.92	91	N/A
0.10	1.56	124	N/A
0.12	2.20	131	0.8
0.15	3.00	152	1.1
0.20	3.81	174	1.4

could result from impact at higher height. At the lowest impact height of 0.05 m, Figure 6(a) shows a peak ΔC of approximately 0.9 pF. The corresponding extent of damage in Figure 6(f) reveals a relatively small localized deformation region, primarily symmetric about the origin without any indentation to the sample. The recorded force by the load cell from Figure 6(k) peaks at around 90 N, occurring over a brief time interval, which aligns with the expected behavior for minimal impact energy. Increasing the height to 0.10 m, the ΔC value shown in Figure 6(b) rises sharply to about 1.5 pF before settling, indicating increased strain response. The damage profile in Figure 6(g) expands, displaying a broader affected area, though still maintaining some symmetry without any indentation on the sample. The load cell force, recorded in Figure 6(l), peaks at approximately 124 N, reflecting the increased energy associated with a higher impact.

At impact height of 0.12 m, the capacitance change in Figure 6(c) reaches a maximum of around 2.2 pF before gradually stabilizing, suggesting further strain development. As illustrated in Figure 6(h), the extent of damage shows noticeable deformation beyond the earlier cases, with a slight asymmetry starting to emerge, introducing an indentation depth of about 0.8 mm. The peak force recorded, shown in Figure 6(m), is about 131 N, almost similar to 0.10 m, likely due to variations in the impact's interaction with the composite. At 0.15 m, the ΔC value in Figure 6(d) exhibits a pronounced peak of around 3.0 pF, demonstrating a significant strain response. The corresponding extent of damage in Figure 6(i) further expands, becoming more irregular and indicating a higher degree of localized damage and indentation depth of 1.1 mm. The load cell data in Figure 6(n) show a peak force of approximately 150 N, consistent with the greater impact energy.

Finally, the highest impact height of 0.20 m results in the largest capacitance change of approximately 3.8 pF, as shown in Figure 6(e). This significant response highlights the extreme strain experienced by the SEC under this condition. The extent of damage in Figure 6(j) displays the most substantial deformation, with a highly irregular shape and large indentation depth of 1.4 mm, suggesting severe localized damage to the composite. The force curve in Figure 6(o) peaks near 170 N, indicating the high energy transfer during the impact. The results demonstrate a clear correlation between impact height and the SEC's capacitance change, extent of damage, and recorded force. Table 1 presents detailed data from the impact test indicating that as impact height increases, all three metrics progressively increase, underscoring the SEC's sensitivity and effectiveness in monitoring impact-induced strain and damage within the sandwich composite structure.

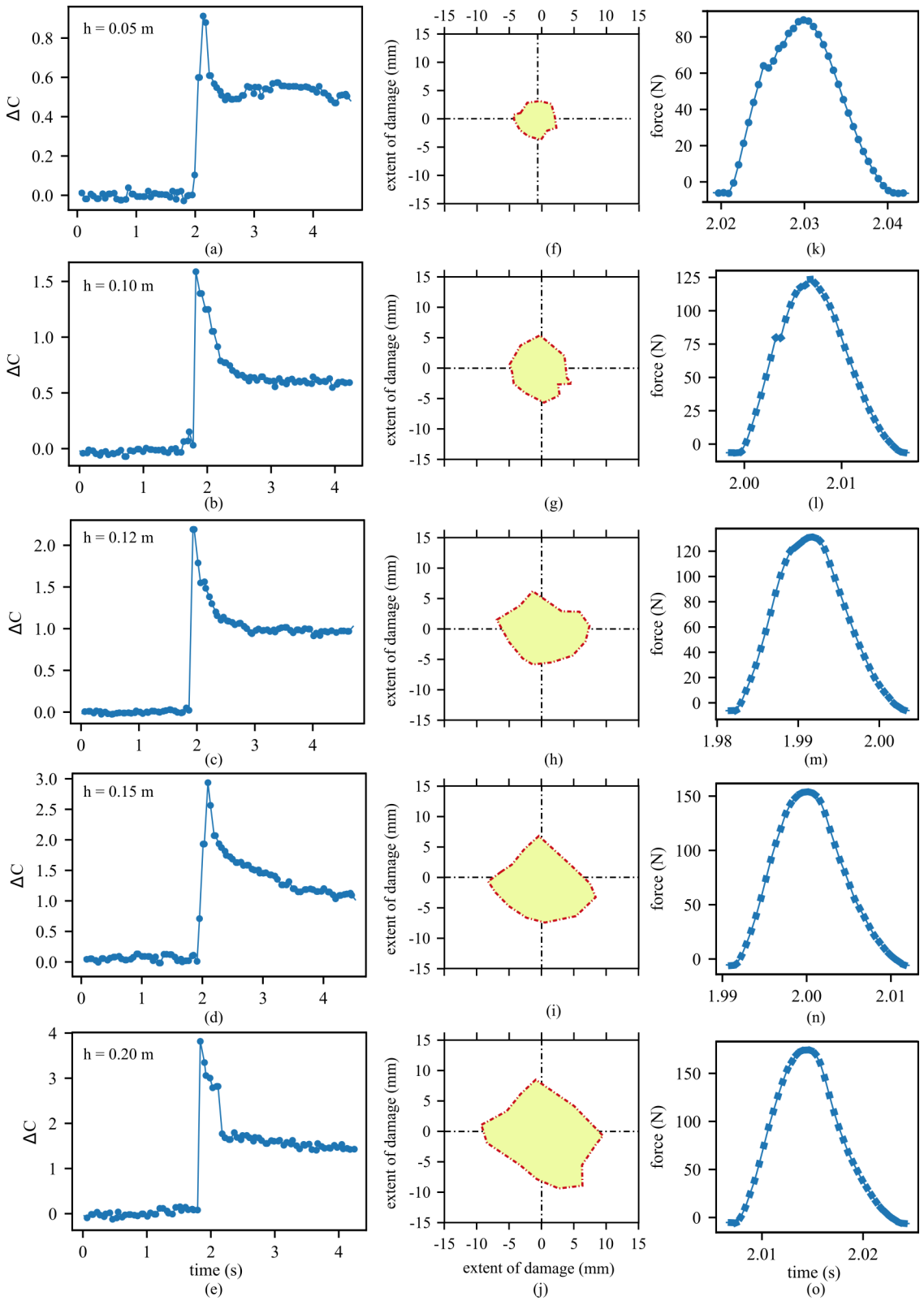

Figure 6. Impact test on sandwich composite with (a) to (e) showing the SEC's capacitance change at different impact heights; (f) to (j) the extent of damage after each impact, and; (k) to (o) the force recorded by the load cell upon impact.

4.3 Impact energy and Energy absorption

The performance of sandwich composites embedded with SEC and battery can be evaluated under controlled impact conditions using the impact energy and energy absorption metrics. The analysis includes impact energy, energy absorption, and their correlation with height and capacitance changes. The impact energy was calculated as the potential energy for the short height considered using the formula $E = mgh$, where m is the mass of the impactor (7.5 kg), g is the acceleration due to gravity (9.81 m/s^2), and h is the height from which the impactor was dropped. As shown in Table 2, impact energy increased linearly with height, reaching a maximum of 14.72 J at a height of 0.20 m, as the impact energy solely depends on the drop's height and the impactor's mass.

Table 2. Impact energy and Energy absorbed by the sandwich composite

Impact Height (m)	Impact energy (J)	ΔC (pF)	Energy absorbed (J)
0.05	3.68	0.92	3.35
0.10	7.36	1.56	6.70
0.12	8.83	2.20	8.03
0.15	11.04	3.00	10.04
0.20	14.72	3.81	13.39

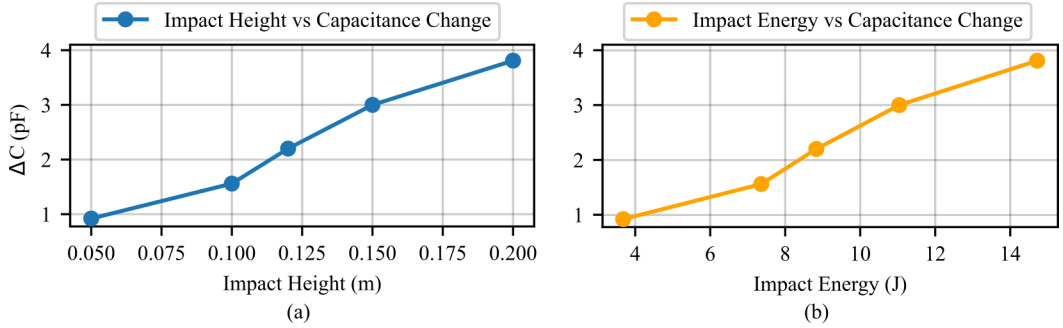

Figure 7. Change in capacitance when subjected to impacts, showing the change in capacitance as a function of (a) impact height, and (b) impact energy.

Figure 7(a) illustrates the relationship between impact height and capacitance change in a sandwich composite, demonstrating a clear positive correlation between the impact height and the resulting change in capacitance. As the impact height increases from 0.05 m to 0.20 m, the capacitance change consistently rises, starting at 0.90 pF and reaching 3.81 pF. This trend indicates that greater impact heights generate larger deformations or stress in the composite, which, in turn, results in more significant changes in capacitance. Figure 7(b) further corroborates this relationship, showing a similar positive trend between impact energy and capacitance change. As the impact energy increases from 3.68 J to 14.72 J, the capacitance change follows an upward trajectory, increasing from 0.92 pF to 3.81 pF. This result suggests that higher energy impacts induce greater mechanical strain in the composite, leading to larger capacitance changes. The results highlight the sensor's sensitivity to mechanical impacts, making it a potential candidate for impact detection or monitoring applications.

Energy absorption values were calculated for composites with embedded SEC and battery. The energy absorbed by the laminate was determined using Equation 8 This formula accounts for the kinetic energy at the point of impact and the potential energy contribution. The data indicates that as the impact height increased, the sandwich composite absorbed more energy while some portion of the impact energy was lost to rebound. Lower impact heights resulted in minimal energy absorption, with negligible structural deformation, whereas higher energy levels (above 11 J) caused significant indentation, material damage and indentation depth. The embedded SEC effectively monitored this behavior, as the capacitance change data demonstrated.

4.4 Charge/Discharge after Impact

Figure 8 presents the charge-discharge performance of a sandwich composite sample with an embedded battery and SEC before and after mechanical impacts from varying heights. The charge-discharge curves show how the battery's electrochemical performance evolves under different impact conditions, with impact heights ranging from 0.05 m to 0.20 m. The label "before impact" represents the baseline performance of the embedded battery, showing a smooth voltage drop during discharge from approximately 4.25 V to 2.75 V over a capacity range of 0 to 600 mAh. This indicates that, before any mechanical stress, the embedded battery exhibits stable behavior with efficient charge-discharge cycles and minimal internal resistance.

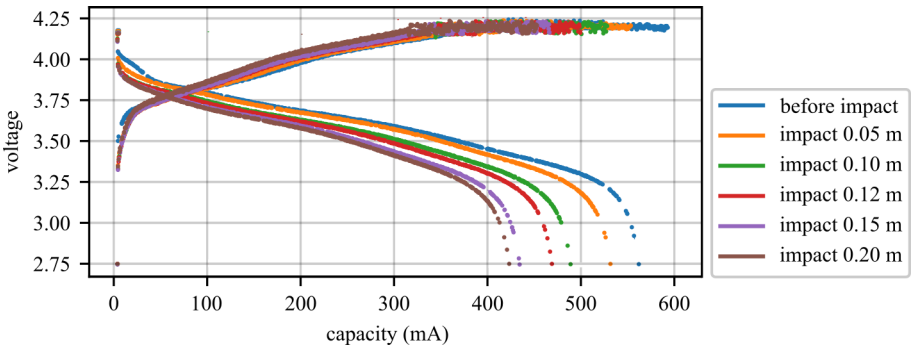

Figure 8. Charge and discharge test on sandwich composite sample with embedded battery and SEC before impact, and after impact height 0.05 m, 0.10 m, 0.12 m, 0.15 m and 0.20 m.

After subjecting the composite sample to mechanical impacts, noticeable deviations from the original curve are observed. At an impact height of 0.05 m, the discharge curve shows a slight deviation from the baseline, with a minor increase in voltage drop during discharge. This suggests that the system experienced minor internal resistance or a slight reduction in capacity, but the overall performance remained relatively stable. As the impact height increased to 0.10 m, the charge-discharge curve began to show more significant deviations. The voltage drop during discharge became more pronounced, indicating that the battery experienced more significant internal damage, likely affecting its capacity retention and efficiency during the charge and discharge phases. Following an impact from a height of 0.12 m, the system's performance showed further deterioration, with the voltage drop becoming steeper and the capacity declining more noticeably. At this stage, the deviation from the baseline curve suggests more substantial damage, potentially involving microstructural changes within the composite sample, such as micro-cracks or delamination of layers contributing to the embedded battery's electrochemical function. At 0.15 m, the damage became more severe, with the discharge curve displaying a rapid drop in voltage and reduced capacity. The charging phase also became less efficient, indicating that the internal components of the embedded system were no longer functioning optimally, potentially due to compromised electrodes or electrolyte pathways. The most significant degradation in performance occurred after an impact height of 0.20 m. The voltage drop during discharge was steep, and the system's capacity was considerably reduced. The recovery during the charging phase was inefficient, with the voltage failing to return to its initial levels. This behavior suggests that the composite sample suffered substantial structural damage, affecting the embedded battery. The high-energy impact likely caused extensive internal fractures or delamination within the composite layers, further increasing internal resistance and reducing the battery's ability to hold and transfer charge effectively.

Lower impact heights, such as 0.05 m and 0.10 m, caused only minor deviations in the charge-discharge curves, suggesting that the embedded system can tolerate low-energy impacts with minimal performance loss within a sandwich composite. However, as the impact height increased beyond 0.12 m, the composite sample exhibited significant reductions in capacity and efficiency, indicating that higher-energy impacts cause progressive structural damage to the embedded components. These results highlight the need for further investigation into the mechanical durability of embedded systems, particularly in applications subjected to repeated or high-energy mechanical stresses.

5. CONCLUSION

This study investigated the application of soft elastomeric capacitors for real-time impact energy monitoring in batteries embedded within sandwich composites. The research demonstrated that SECs effectively detect and quantify impact energy while maintaining embedded batteries' structural and electrochemical integrity. Experimental results showed a clear correlation between SEC capacitance changes and impact energy levels. At an impact height of 0.05 m (3.7 J), the SEC exhibited a capacitance change of 0.9 pF with minimal structural damage, while higher impact heights of 0.15 m (11 J) and 0.20 m (14.7 J) resulted in capacitance changes of 2.20 pF and 3.0 pF, respectively, with increasing structural damage and indentation depths of up to 1.4 mm. The study further revealed that low-energy impacts $< 7.4J$ caused negligible deviations in the charge-discharge performance of the embedded battery, highlighting the feasibility of integrating SECs for multifunctional composite applications. These findings underscore the potential of SECs to enhance safety in high-risk applications, such as aerospace, electric vehicles, and renewable energy systems, by providing real-time impact monitoring and early damage detection. While the results affirm the effectiveness of SECs in impact energy monitoring, further testing under varied environmental conditions and repeated impact scenarios is left for future studies to assess long-term durability and scalability.

ACKNOWLEDGMENTS

The authors gratefully acknowledge the financial support of the Departments of Transportation of Iowa, Kansas, South Carolina, and North Carolina, through the Transportation Pooled Fund Study TPF-5(449).

REFERENCES

[1] Viswanathan, V., Epstein, A. H., Chiang, Y.-M., Takeuchi, E., Bradley, M., Langford, J., and Winter, M., "The challenges and opportunities of battery-powered flight," Nature **601**(7894), 519–525 (2022).

[2] Liu, S., Zhang, G., and Wang, C.-Y., "Challenges and innovations of lithium-ion battery thermal management under extreme conditions: A review," ASME Journal of Heat and Mass Transfer **145**(8), 080801 (2023).

[3] Chen, M., Zhang, Y., Xing, G., Chou, S.-L., and Tang, Y., "Electrochemical energy storage devices working in extreme conditions," Energy & Environmental Science **14**(6), 3323–3351 (2021).

[4] Li, H., Zhou, D., Cao, J., Li, Z., and Zhang, C., "On the damage and performance degradation of multifunctional sandwich structure embedded with lithium-ion batteries under impact loading," Journal of Power Sources **581**, 233509 (2023).

[5] Nagavally, R. R., "Composite materials-history, types, fabrication techniques, advantages, and applications," Int. J. Mech. Prod. Eng **5**(9), 82–87 (2017).

[6] Hsissou, R., Seghiri, R., Benzekri, Z., Hilali, M., Rafik, M., and Elharfi, A., "Polymer composite materials: A comprehensive review," Composite structures **262**, 113640 (2021).

[7] Pattarakunnan, K., Galos, J., Das, R., and Mouritz, A., "Impact damage tolerance of energy storage composite structures containing lithium-ion polymer batteries," Composite Structures **267**, 113845 (2021).

[8] Kon, S., Oldham, K., and Horowitz, R., "Piezoresistive and piezoelectric mems strain sensors for vibration detection," in [Sensors and Smart Structures Technologies for Civil, Mechanical, and Aerospace Systems 2007], **6529**, 898–908, SPIE (2007).

[9] Laflamme, S., Ubertini, F., Saleem, H., D'Alessandro, A., Downey, A., Ceylan, H., and Materazzi, A. L., "Dynamic characterization of a soft elastomeric capacitor for structural health monitoring," Journal of Structural Engineering **141**(8), 04014186 (2015).

[10] Rácz, Z., Hackney, E. M., and Wood, D., "Soft elastomeric capacitive sensor for structural health monitoring," Procedia Engineering **168**, 721–724 (2016).

[11] Ogunniyia, E., Liub, H., Whitea, J., Downeya, A. R., Laflammeb, S., Lie, J., Bennette, C., Collinse, W., Jof, H., and Ziehlc, P., "Performance evaluation of flexible capacitive sensors on non-uniform surfaces," in [Proc. of SPIE Vol], **12949**, 1294916–1.

[12] Vereen, A., Downey, A. R., Sockalingam, S., and Laflamme, S., "Validation of large area capacitive sensors for impact damage assessment," Measurement Science and Technology **35**(3), 035106 (2023).

[13] Li, R., Li, W., Singh, A., Ren, D., Hou, Z., and Ouyang, M., "Effect of external pressure and internal stress on battery performance and lifespan," Energy Storage Materials **52**, 395–429 (2022).

[14] See, K., Wang, G., Zhang, Y., Wang, Y., Meng, L., Gu, X., Zhang, N., Lim, K., Zhao, L., and Xie, B., "Critical review and functional safety of a battery management system for large-scale lithium-ion battery pack technologies," International Journal of Coal Science & Technology **9**(1), 36 (2022).

[15] Galos, J., Best, A., and Mouritz, A., "Multifunctional sandwich composites containing embedded lithium-ion polymer batteries under bending loads," Materials & Design **185**, 108228 (2020).

[16] Pattarakunnan, K., Galos, J., Das, R., and Mouritz, A., "Tensile properties of multifunctional composites embedded with lithium-ion polymer batteries," Composites Part A: Applied Science and Manufacturing **136**, 105966 (2020).

[17] Wang, Y., Peng, C., and Zhang, W., "Mechanical and electrical behavior of a novel satellite multifunctional structural battery," (2014).

[18] Shalouf, S. M., Zhang, J., and Wang, C., "Effects of mechanical deformation on electric performance of rechargeable batteries embedded in load carrying composite structures," Plastics, Rubber and Composites **43**(3), 98–104 (2014).

[19] Galos, J., Pattarakunnan, K., Best, A. S., Kyratzis, I. L., Wang, C.-H., and Mouritz, A. P., "Energy storage structural composites with integrated lithium-ion batteries: a review," Advanced Materials Technologies **6**(8), 2001059 (2021).

[20] Ladpli, P., Nardari, R., Kopsaftopoulos, F., and Chang, F.-K., "Multifunctional energy storage composite structures with embedded lithium-ion batteries," Journal of Power Sources **414**, 517–529 (2019).

[21] Asp, L. E. and Greenhalgh, E. S., "Structural power composites," Composites science and technology **101**, 41–61 (2014).

[22] Downey, A., Pisello, A. L., Fortunati, E., Fabiani, C., Luzi, F., Torre, L., Ubertini, F., and Laflamme, S., "Durability and weatherability of a styrene-ethylene-butylene-styrene (sebs) block copolymer-based sensing skin for civil infrastructure applications," Sensors and Actuators A: Physical **293**, 269–280 (2019).

[23] Liu, H., Laflamme, S., Li, J., Downey, A., Bennett, C., Collins, W., Ziehl, P., Jo, H., and Todsen, M., "Sensing skin technology for fatigue crack monitoring of steel bridges: Laboratory development, field validation, and future directions," International Journal of Bridge Engineering, Management and Research **1** (Sept. 2024).

[24] Ogunniyi, E., Vareen, A., Downey, A. R., Laflamme, S., Li, J., Bennett, C., Collins, W., Jo, H., Henderson, A., and Ziehl, P., "Investigation of electrically isolated capacitive sensing skins on concrete to reduce structure/sensor capacitive coupling," Measurement Science and Technology **34**(5), 055113 (2023).

[25] Liu, H., Laflamme, S., Li, J., Bennett, C., Collins, W. N., Downey, A., Ziehl, P., and Jo, H., "Soft elastomeric capacitor for angular rotation sensing in steel components," Sensors **21**(21), 7017 (2021).

[26] D7136/D7136M, D., "Standard test method for measuring the damage resistance of a fiber-reinforced polymer matrix composite to a drop-weight impact event," ASTM International (2017).